




## Valley-orbit splitting of lithium-related donors in silicon

S. G. Pavlov <sup>1</sup>, N. V. Abrosimov <sup>2</sup>, and H.-W. Hübers <sup>1,3</sup><sup>1</sup>*Institute of Optical Sensor Systems, German Aerospace Center (DLR), Rutherfordstr. 2, 12489 Berlin, Germany*<sup>2</sup>*Leibniz-Institut für Kristallzüchtung (IKZ), Max-Born-Str. 2, 12489 Berlin, Germany*<sup>3</sup>*Department of Physics, Humboldt-Universität zu Berlin, Newtonstr. 15, 12489 Berlin, Germany*

(Received 5 January 2023; accepted 23 February 2023; published 20 March 2023)

The energy spectra of lithium-related donors in silicon are revisited by temperature-dependent infrared absorption spectroscopy. We determine the valley-orbit splitting of an interstitial isolated lithium donor and its complex with residual oxygen in float-zone grown crystals doped from the melt. Lithium-oxygen donors exhibit a temperature evolution of their absorption spectra similar to that of substitutional single-electron group-V donors, while its valley-orbit splitting is corrected upwards to +9.865(5) meV. For the lithium donor, the previously reported inverted valley-orbit splitting is not confirmed since the components of different symmetry are not spectrally resolved in our study. Instead, the chemical shift of the ground state of the donor, having a symmetry different from that of group-V donors, was corrected to a slightly larger value of 1.82(2) meV. Intracenter transitions from the split-off ground state of the Li donor exhibit an anomalous broadening. In addition, several Rydberg-like high excited states, up to  $7h_{\pm}$ , of lithium-related centers were determined from absorption spectra of moderately doped samples.

DOI: [10.1103/PhysRevB.107.115205](https://doi.org/10.1103/PhysRevB.107.115205)

## I. INTRODUCTION

The interstitial electrically active lithium (Li) center in silicon (Si) is one of the most spectacular shallow donors. It has been known for more than fifty years and, despite that, various concepts for the description of its energy spectra appeared and the issue is not completely resolved to date. This is partly due to technological challenges regarding the production of high-quality Si:Li crystals with reproducible and well-controlled properties as required for research. Usually, Si:Li crystals have a few Li-related donor types, which complicates the interpretation of its energy spectra.

Electrically active interstitial impurities in semiconductors are usually formed by light atoms (Li, Mg), which have a high inherent mobility in the crystal lattice. Such a mobility predetermines large diffusion coefficients of interstitials and their ability to move inside the crystal and to form complexes with other chemical impurities present in the crystal. Energy spectra as well as optical and electrical properties of interstitials depend strongly on the position of the impurity atom relative to the nearest atoms in the host lattice. They can obey either tetrahedral or hexagonal/trigonal-type symmetry in cubic/diamond-type lattices. In the cubic (tetrahedral)  $T_d$  symmetry group the sixfold-degenerated  $1s$  ground state of a donor in Si decomposes due to valley-orbit splitting (VOS) into singlet  $A_1$  ( $s$  type, other notation is  $\Gamma_1$ ), doublet  $E$  ( $d$  type,  $\Gamma_3$ ), and triplet  $T_2$  ( $p$  type,  $\Gamma_5$ ) states, with the  $1s(A_1)$  level being most downshifted from the  $1s(E)$  level [1]. The latter has the smallest chemical shift and a binding energy which is closest to that obtained by the effective mass (EMT) approximation [2]. The VOS energy for such split- $T_d$  centers is defined as the energy gap between the levels with the largest separation, namely the  $1s(A_1)$  and the  $1s(E)$  levels. In the hexagonal symmetry, a  $T_2$  triplet splits further into singlet

and doublet states. Similarly, trigonal symmetry reduces the state degeneracy further: For instance, a centrosymmetric  $D_{3d}$  symmetry reduces the  $1s$  state into two singlets and two doublets [3].

In electron spin resonance (ESR) experiments Feher [4] has observed an anisotropy of the  $g$  value of a donor in a Si:Li crystal at lattice temperature 1.5 K (Li was diffused in the “pulled” Si crystal; concentration of Li  $\cong 3 \times 10^{16} \text{ cm}^{-3}$ ; of oxygen  $\sim 10^{16} \text{ cm}^{-3}$ ). He concluded that the electronic wave function of interstitial Li does not have tetrahedral symmetry, unlike that of group-V substitutional donors in Si. He also supposed that Li may occupy a position along the [111] axis between the 000 and 333 positions in the unit cell [4]. Also, the fine structure of the ground state has been observed and assigned to a Li-isotope related splitting. Since no ESR signal was observed when Li was diffused into a float-zone grown Si crystal, Feher assumed that paramagnetic resonance should be assigned to the lithium-oxygen complex (Li-O) [4].

Aggarwal *et al.* [5] studied Li and Li-O donors by infrared absorption and piezospectroscopy in floating-zone (FZ, low oxygen) and crucible-grown [i.e., Czochralski (Cz) technique, inherent high oxygen in crystals] Si samples. To dope Si with Li, Li dispersed in mineral oil was diffused for 2 h in a helium atmosphere at 200° C, with further heat treatment at 600° C for 2 h in order to increase the homogeneity of Li in the crystal. The Li-O transitions were not resolved in FZ-grown Si:Li (donor concentration  $\cong 1 \times 10^{15} \text{ cm}^{-3}$ ) but were observed in crucible-grown Si:Li (concentration of donors  $\cong 6 \times 10^{15} \text{ cm}^{-3}$ ; of oxygen  $\sim 5 \times 10^{17} \text{ cm}^{-3}$ ) [5]. From analysis of the impurity spectra of Si:Li under stress, the authors concluded that the number of split components indicates that isolated Li occupies a tetrahedral site with the ground state composed of unresolved doublet and triplet  $1s(E + T_2)$  states with the singlet  $1s(A_1)$  state above. In the same way as

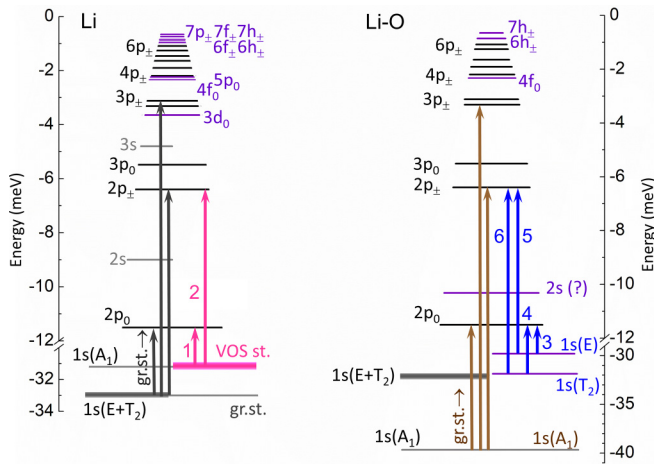


FIG. 1. Schematic presentation of the energy structure of the isolated Li donor and Li-O donor complex in Si and types of observed optical intracenter transitions. Black lines are for discrete states whose assignments in previous publications (see Tables I and III) coincide with this work. Gray lines are previously reported states and violet lines are the states which are redetermined or which are resolved in this work (see Table III). The energies of the states are given relative to the conduction band bottom, which is taken as zero. Arrows with “gr.st. →” represent transition series from the donor ground state. Lines 1 and 2 are observed thermally induced transitions from Li VOS states. Lines 3–6 are observed thermally induced transitions from Li-O VOS states.

for group-V donors, the selection rules for splitting under stress identifies the Li-O center as a hydrogen-like center of  $T_d$  symmetry with a  $1s(A_1)$  ground state. The VOS energy between these states was derived from assignment of specific lines emerging with increasing lattice temperature. The absorption line at 24.80(5) meV, which is pronounced in the spectra at  $\sim 20$  K, was assigned to the  $1s(A_1) \rightarrow 2p_{\pm}$  transition of the Li donor. The line at 25.60(5) meV, also pronounced in the absorption spectra at  $\sim 20$  K, was assigned to the  $1s(E+T_1) \rightarrow 2p_{\pm}$  transition of the Li-O donor. By this, the authors determined the VOS of the isolated Li donor as  $-1.8(1)$  meV, meaning that the  $1s(A_1)$  singlet state is “inverted” to the  $1s(E)$  state. For an isolated Li-O donor complex the determined VOS was  $+7.7(1)$  meV, meaning that it is a group-V-like ground state (assigned to have also tetrahedral symmetry in Si) [5]. Note that these assignments of the ground-state levels for both Li-related donors (see Fig. 1 and Table I) still exist today.

Further Li-O complexes with ionization energies between 34.9 and 39.2 meV were observed by Gilmer *et al.* [6] in Si doped by Li under diffusion from a tin bath containing 0.25% Li for 23 h at 730 K. They assigned the  $\sim 25$  meV spectral feature to a Li transition terminating in the  $2s$  Li state and concluded that the sixfold degeneracy of the  $1s$  ground has not been lifted because of a missing second series of thermally induced transitions (if VOS is small), while a sample temperature of about 20 K was already sufficient to detect this effect.

A theoretical model of the inverted ground state of isolated Li in Si has been proposed and exploited by Nara and Morita [3]. The authors calculated dependences of chemical shifts of the ground-state components due to dielectric screening

of the impurity potential on distances between interstitial and host atoms. They showed that the trigonal  $D_{3d}$  – site symmetry for the Li donor favors an inverted group-V-like ground state when compared with the tetragonal site symmetry  $T_d$ . They concluded that the energy gaps would fit to the lowest ground state, that is, the nearly degenerate multiple (fivefold)  $1s (A_{2u} + E_g + E_u)$  state with an ionization energy of 30 meV, lying  $\sim 1.5$  meV below the fully symmetric singlet  $1s (A_{1g})$  state [3].

ESR studies by Watkins and Ham [7] on Si:Li samples made from the material of Ref. [5], confirmed the complexity of the energy structure of Li in Si, obviously exhibiting degeneration of its ground-state orbitals. They assumed a tetrahedral rather than a hexagonal site of isolated Li, which might be slightly displaced from the tetrahedral site. The authors presented arguments for the  $^7\text{Li}$  hyperfine-interaction splitting, that would give a VOS of  $\sim 1.8$  meV.

Jagannath *et al.* [8,9] have revisited infrared absorption spectra of less-doped Si:Li samples (donor concentration  $\sim 5\text{--}11 \times 10^{14} \text{ cm}^{-3}$ ) with higher spectral resolution of their Fourier-transform spectrometer ( $\sim 0.06\text{--}0.28 \text{ cm}^{-1}$ ) compared to Ref. [5] with a grating spectrometer. In these samples they found simultaneous presence of both isolated Li and Li-O donors, in both types of Si crystals: FZ and crucible grown. From the piezospectroscopic data they confirmed the uplifted  $1s(A_1)$  state of isolated Li. They proposed a correction to the VOS of  $-1.78$  meV (see Table I) and they observed a few weak transitions in Li and Li-O impurity spectra (see Table III), as well as a series of hydrogen-like centers with binding energies between those for isolated Li and Li-O.

Another theoretical model was reported by Szablak and Altarelli [10]. They introduced an additional short-range  $\text{Li}^+$  Coulomb pseudopotential that allowed obtaining solutions with the  $A_1$  state having the lowest binding energy (29.6 meV) followed by the  $E$  (30.7 meV) and  $T_2$  (31.2 meV) levels.

A low-temperature (1.8 K) spectroscopic study of residual Li (estimated concentration  $\sim 1 \times 10^{14} \text{ cm}^{-3}$ ) in FZ-grown isotopically enriched  $^{28}\text{Si}$  crystals [13] revealed Li-related donor transitions with a fine splitting  $\sim 0.06 \text{ cm}^{-1}$  of all  $s \rightarrow p$  type transitions, which is smaller than the fine splitting in natural Si. It was assumed to be related to the splitting of the Li ground state, assigned to the splitting of  $1s (\Gamma_3)$  and  $1s (\Gamma_5)$  states. Also, a VOS of the  $2p_0$  state ( $\sim 7 \mu\text{eV}$ ) was assumed for the additional structure of the ground state  $\rightarrow 2p_0$  transition [13].

Spin-orbit coupling of Li and Li-O ground states has been investigated in a series of ESR studies in  $^{28}\text{Si}:\text{Li}$  by Ezhevskii *et al.* and found to be 1 and 15  $\mu\text{eV}$ , correspondingly [14].

We report detailed temperature-dependent absorption spectra of FZ-grown Si doped by Li from the melt using the pedestal technique. Differences in the temperature evolution of the impurity transitions allowed us to distinguish between the energy structure of isolated Li and Li-O complex donors. For the isolated Li center, we find the structure of the ground states different from those reported in previous studies. For the Li-O donor complex, we determine the energy splitting between valley-orbit split states and correct the VOS energy using the asymptotic behavior of temperature evolution of the respective intracenter transitions. Finally, the energies of several excited states were experimentally determined from

TABLE I. Assignment and experimental binding energy of the VOS ground states of isolated Li and Li-O complex donors in Si (gr. st. : ground state, ex. st. : excited state).

Donor	VOS splitting (meV)	Assignment of ground state and its binding energy (meV)		
		Ground state		Excited states
Li		32.5 <sup>b</sup>		<i>Not observed</i>
	-1.8(1) <sup>a</sup>	1s( $E + T_1$ ) <i>fivefold deg.</i> :		
	-1.78(2) <sup>d</sup>	32.81(6) <sup>a</sup>		1s( $A_1$ ) <i>singlet</i> <sup>a,d</sup>
	-1.76(4) <sup>c</sup>	33.02 <sup>d</sup>		
		33.03 <sup>e</sup>		
		33.00 <sup>f</sup>		
Li-O	1.82(2) between gr.st. and ex. st.	33.009(5)		<i>Unresolved</i>
		39.2 <sup>b</sup>		
		1s( $A_1$ ) <i>singlet</i> :		<i>Unresolved</i> 1s( $E + T_2$ )
	+7.7(1) <sup>a</sup>	39.41(7) <sup>a</sup>		32.00 <sup>d</sup>
	+7.67 <sup>d</sup>	39.67 <sup>d</sup>		
		39.67 <sup>f</sup>		
	+9.865(5)	1s( $A_1$ ) <i>singlet</i> :	1s( $E$ )	1s( $T_2$ )
		39.669(5)	29.804(5)	31.87(1)

<sup>a</sup>Diffusion doping of Li in FZ- and Cz-grown Si crystals [5]; absorption (Si sample is attached to a copper tail piece which is in contact with liquid He and H<sub>2</sub> coolants) and piezo-optical (Si sample is constrained in a copper jig attached to the copper tail in optical cryostat) spectroscopy using the Perkin-Elmer grating spectrometer.

<sup>b</sup>Diffusion doping of Li in FZ- and Cz-grown Si crystals [6]; absorption (Si sample is attached to a cold finger with a contact to liquid He bath; temperature on the Ge thermistor with a contact to the Si:Li sample bottom was ~20 K); grating spectrometer with standard error in spectral resolution of 0.03 meV.

<sup>c</sup>Diffusion doping of Li in Fz- and Cz-grown Si crystals as in [5]; piezo-spectroscopy using the Fourier-transform spectrometer with resolution of 0.025 cm<sup>-1</sup> [8].

<sup>d</sup>Diffusion doping of Li in Fz- and Cz-grown Si crystals [9]; absorption (Si sample is attached to a copper tail piece with GE 7031 at the bottom edge of the sample; the copper holder is in contact with liquid He and H<sub>2</sub> coolants) and piezo-optical (the same mounting as in [5]) spectroscopy using the Fourier-transform spectrometer with resolution of 0.06 cm<sup>-1</sup>.

<sup>e</sup>Li-doped Si crystals [11]; photoluminescence spectroscopy; pumped liquid He temperature.

<sup>f</sup>Residual Li-related donors [12] (estimated concentration of Li is about 10<sup>10</sup> cm<sup>-3</sup>) in undoped high-resistivity Si; measured at 11-17 K; photothermal ionization spectroscopy with the Fourier-transform spectrometers having resolution up to 0.06 cm<sup>-1</sup>.

TABLE II. Parameters of the investigated Si:Li samples and detected transitions from the excited VOS states of isolated Li and Li-O complex donors. Accuracy of concentration is about 10%. First three digits after V numbers the original Si:Li crystal ingot. Concentration of the main abundant donors in the samples was derived from room-temperature resistivity (taken as total concentration of donors) using the approach of the rule of sum with variables weighted by the oscillator strengths of certain intracenter transitions, similar to the approach in Ref. [16].

Sample No.	Mean thick-ness (mm)	Concentrations of donors (cm <sup>-3</sup> )			Observed transitions from thermally populated VOS states					
					Li VOS →		Li-O 1s( $E$ ) →		1s( $T_2$ ) →	
		Li	Li-O	P	2p <sub>0</sub>	2p <sub>±</sub>	2p <sub>0</sub>	2p <sub>±</sub>	2p <sub>0</sub>	2p <sub>±</sub>
2V3951A	0.134	2.7 × 10 <sup>13</sup>	1.6 × 10 <sup>12</sup>	2. × 10 <sup>11</sup>						
2V3951E	0.135	2.6 × 10 <sup>13</sup>	2.1 × 10 <sup>12</sup>	6. × 10 <sup>11</sup>						
V467-1	0.058	1.1 × 10 <sup>15</sup>	8.9 × 10 <sup>13</sup>	8 × 10 <sup>11</sup>		X		X		X
V467-2	0.055	1.1 × 10 <sup>15</sup>	1.3 × 10 <sup>14</sup>	9. × 10 <sup>11</sup>		X		X		X
V467-3	0.098	1.7 × 10 <sup>15</sup>	2.1 × 10 <sup>14</sup>	2 × 10 <sup>12</sup>	X	X		X		X
V467-4	0.097	1.7 × 10 <sup>15</sup>	2.1 × 10 <sup>14</sup>	2 × 10 <sup>12</sup>	X	X	X	X	X	X
V471-1	0.056	2.9 × 10 <sup>15</sup>	4.5 × 10 <sup>14</sup>	1.5 × 10 <sup>12</sup>	X	X		X		X
V471-2	0.056	2.8 × 10 <sup>15</sup>	5.8 × 10 <sup>14</sup>	2.0 × 10 <sup>12</sup>	X	X		X		X
V471-3	0.099	2.9 × 10 <sup>15</sup>	4.8 × 10 <sup>14</sup>	2 × 10 <sup>12</sup>	X	X		X	X	X
V482-3	0.087	5.4 × 10 <sup>15</sup>	8.9 × 10 <sup>13</sup>	2.6 × 10 <sup>12</sup>	X	X	X	X	X	X
V482-4	0.098	5.3 × 10 <sup>15</sup>	8.9 × 10 <sup>13</sup>	1.6 × 10 <sup>12</sup>	X	X		X	X	X

TABLE III. Energies of the observed impurity transitions of Li-related donors in Si and assigned types of the respective states. Energies of weak and moderate transitions are derived from the absorption spectra of the Si:Li No. 467 samples. Values in  $\text{cm}^{-1}$  are the peak positions of the transitions from the transmission spectrum of the sample No. 467-4, the values in meV are the mean values of the No. 467 series and of the thermally excited transitions from the Si:Li No. 471 series. For the strongest transitions, saturated in high-doped samples, the transition energies are given as they are in the low-doped samples Si:Li No. 482 2V3951 series, marked with \*. Energy accuracy is  $3 \mu\text{eV}$ . VOS stays for the lowest excited state(s). Accuracy of the transition's energy is  $5 \mu\text{eV}$ , unless a different value is given.

Donor lines (meV) & in $\text{cm}^{-1}$		Transition/Line/Band assignment	Transition/Line/Band assignment and energy	
@5K	@ 20K / @ 35 K	(this work) Li	(previous reports)	
19.69(2)	19.70(2) /	VOS $\rightarrow 2p_0$		
158.80 $\text{cm}^{-1}$	19.70(2)			
21.50*	21.49 /	1s gr.st. $\rightarrow 2p_0$	gr.st. $\rightarrow 2p_0$	21.49 [12]
173.45 $\text{cm}^{-1}$	21.47			21.505(1) [13]
			1s(E + T <sub>1</sub> ) $\rightarrow 2p_0$	21.50(2) [5]
			1s(E + T <sub>2</sub> ) $\rightarrow 2p_0$	21.51 [9]
24.78(2)	24.79 /	VOS $\rightarrow 2p_{\pm}$	1s(A <sub>1</sub> ) $\rightarrow 2p_{\pm}$	24.80(5) [5]
199.89 $\text{cm}^{-1}$	24.79		1s(A <sub>1</sub> ) $\rightarrow 2s$	[6]
			gr.st. $\rightarrow 2p_{\pm}$	26.60 [12]
26.62*	26.61 /	1s gr.st. $\rightarrow 2p_{\pm}$		26.615(1) [13]
214.66 $\text{cm}^{-1}$	26.59		1s(E + T <sub>1</sub> ) $\rightarrow 2p_{\pm}$	26.63(2) [5]
			1s(E + T <sub>2</sub> ) $\rightarrow 2p_{\pm}$	26.62 [9]
27.52	27.51 /	1s gr.st. $\rightarrow 3p_0$	1s(E + T <sub>1</sub> ) $\rightarrow 3p_0$	27.51(2) [5]
221.98 $\text{cm}^{-1}$	27.49		1s(E + T <sub>2</sub> ) $\rightarrow 3p_0$	27.53 [9]
29.36	29.35 /	1s gr.st. $\rightarrow 3d_0$		
236.82 $\text{cm}^{-1}$				
29.70	29.68 /	1s gr.st. $\rightarrow 4p_0$	1s(E + T <sub>1</sub> ) $\rightarrow 4p_0$	29.72(2) [5]
239.51 $\text{cm}^{-1}$			1s(E + T <sub>2</sub> ) $\rightarrow 4p_0$	29.70 [9]
29.89*	29.88 /		gr.st. $\rightarrow 3p_{\pm}$	29.88 [12]
241.07 $\text{cm}^{-1}$	29.85	1s gr.st. $\rightarrow 3p_{\pm}$	1s(E + T <sub>1</sub> ) $\rightarrow 3p_{\pm}$	29.91(2) [5]
			1s(E + T <sub>2</sub> ) $\rightarrow 3p_{\pm}$	29.90 [9]
30.67	30.68 /	1s gr.st. $\rightarrow 4f_0$		
30.77		1s gr.st. $\rightarrow 5p_0$		
			gr.st. $\rightarrow 4p_{\pm}$	30.81 [12]
30.82*	30.81 /	1s gr.st. $\rightarrow 4p_{\pm}$		30.816(1) [13]
248.55 $\text{cm}^{-1}$	30.79		1s(E + T <sub>1</sub> ) $\rightarrow 4p_{\pm}, 5p$	30.82(2) [5]
			1s(E + T <sub>2</sub> ) $\rightarrow 4p_{\pm}, 5p$	30.82 [9]
			gr.st. $\rightarrow 4f_{\pm}$	31.10 [12]
31.11	31.10 /	1s gr.st. $\rightarrow 4f_{\pm}$	Line b	31.12(2) [5]
250.94 $\text{cm}^{-1}$			1s(E + T <sub>2</sub> ) $\rightarrow 4f_{\pm}$	31.12 [9]
31.37	31.36 /	1s gr.st. $\rightarrow 5f_0$	1s(E + T <sub>2</sub> ) $\rightarrow 5f_0$	31.38 [9]
252.98 $\text{cm}^{-1}$				
31.46		1s gr.st. $\rightarrow 6p_0$		
253.70 $\text{cm}^{-1}$			gr.st. $\rightarrow 5p_{\pm}$	31.54 [12]
31.55	31.539 /	1s gr.st. $\rightarrow 5p_{\pm}$	1s(E + T <sub>1</sub> ) $\rightarrow 5p_{\pm}$	31.56(2) [5]
254.46 $\text{cm}^{-1}$			1s(E + T <sub>2</sub> ) $\rightarrow 5p_{\pm}$	31.55 [9]
31.75	31.740 /	1s gr.st. $\rightarrow 5f_{\pm}$	1s(E + T <sub>1</sub> ) $\rightarrow 5f_{\pm}$	31.77 [9]
256.08 $\text{cm}^{-1}$				
31.80	31.80 /			
256.46 $\text{cm}^{-1}$	31.81			
31.92			gr.st. $\rightarrow 6p_{\pm}$	31.91 [12]
257.50 $\text{cm}^{-1}$	31.91 /	1s gr.st. $\rightarrow 6p_{\pm}$	Line b	31.94(2) [5]
			1s(E + T <sub>2</sub> ) $\rightarrow 6p_{\pm}$	31.95 [9]
32.05		1s gr.st. $\rightarrow 6f_{\pm}$		

TABLE III. (*Continued.*)

Donor lines (meV) & in $\text{cm}^{-1}$		Transition/Line/Band assignment	Transition/Line/Band assignment and energy	
@5K	@ 20K / @ 35 K	(this work) Li	(previous reports)	
258.52 $\text{cm}^{-1}$				
32.12		1s gr.st. $\rightarrow$ 6h $_{\pm}$		
259.07 $\text{cm}^{-1}$				
32.16		1s gr.st. $\rightarrow$ 7p $_{\pm}$	Line c	32.16(2) [5]
259.43 $\text{cm}^{-1}$				
32.24		1s gr.st. $\rightarrow$ 7f $_{\pm}$		
259.98 $\text{cm}^{-1}$				
32.35		1s gr.st. $\rightarrow$ 7h $_{\pm}$		
263.14 $\text{cm}^{-1}$				
				32.81(6) [5]
33.01			Ei	33.00 [12]
				33.02 [9]
				33.03 [11]
		Li-O		
	18.44 / 18.46	1s(E) $\rightarrow$ 2p $_0$		
20.41	20.40 /	1s(T $_2$ ) $\rightarrow$ 2p $_0$		
164.65 $\text{cm}^{-1}$	20.38			
23.51	23.54 /			
189.62 $\text{cm}^{-1}$	23.58	1s(E) $\rightarrow$ 2p $_{\pm}$		
	190.19 $\text{cm}^{-1}$			
25.60	/ 25.58		1s(E + T $_1$ ) $\rightarrow$ 2p $_{\pm}$	25.60(5) [5]
206.46 $\text{cm}^{-1}$	206.3 $\text{cm}^{-1}$	1s(T $_2$ ) $\rightarrow$ 2p $_{\pm}$	1s(E + T $_2$ ) $\rightarrow$ 2p $_{\pm}$	25.60 [9]
28.08				
226.44 $\text{cm}^{-1}$				
28.12	28.12 /	1s(A $_1$ ) $\rightarrow$ 2p $_0$	1s(A $_1$ ) $\rightarrow$ 2p $_0$	28.10(3) [5]
226.64 $\text{cm}^{-1}$	28.15			28.10 [9]
28.86(1)		1s(A $_1$ ) $\rightarrow$ 2s (?)		
232.8(1) $\text{cm}^{-1}$				
33.24				
33.28	33.30 /		gr.st. $\rightarrow$ 2p $_{\pm}$	33.278 [12]
268.37 $\text{cm}^{-1}$	33.33	1s(A $_1$ ) $\rightarrow$ 2p $_{\pm}$	1s(A $_1$ ) $\rightarrow$ 2p $_{\pm}$	33.33(3) [5]
				33.27 [9]
33.30				
34.16	34.17 /	1s(A $_1$ ) $\rightarrow$ 3p $_0$	1s(A $_1$ ) $\rightarrow$ 3p $_0$	34.14(3) [5]
275.56 $\text{cm}^{-1}$				34.16 [9]
36.35	36.37 /	1s(A $_1$ ) $\rightarrow$ 4p $_0$	1s(A $_1$ ) $\rightarrow$ 4p $_0$	36.35(4) [5]
293.18 $\text{cm}^{-1}$				36.34 [9]
36.55	36.57 /	1s(A $_1$ ) $\rightarrow$ 3p $_{\pm}$	gr.st. $\rightarrow$ 3p $_{\pm}$	36.55 [12]
294.78 $\text{cm}^{-1}$	36.59		1s(A $_1$ ) $\rightarrow$ 3p $_{\pm}$	36.51(2) [5]
				36.55 [9]
36.73	36.73 /			
296.25 $\text{cm}^{-1}$	36.74			
37.34		1s(A $_1$ ) $\rightarrow$ 4f $_0$		
301.19 $\text{cm}^{-1}$				
37.48	37.49 /		gr.st. $\rightarrow$ 4p $_{\pm}$ , 5p $_0$	37.48 [12]
302.23 $\text{cm}^{-1}$	37.52	1s(A $_1$ ) $\rightarrow$ 4p $_{\pm}$	1s(A $_1$ ) $\rightarrow$ 4p $_{\pm}$ , 5p $_0$	37.47(3) [5]
				37.47 [9]
37.76	37.79 /		gr.st. $\rightarrow$ 4f $_{\pm}$	37.767 [12]
304.54 $\text{cm}^{-1}$		1s(A $_1$ ) $\rightarrow$ 4f $_{\pm}$	1s(A $_1$ ) $\rightarrow$ 4f $_{\pm}$	37.77 [9]
38.02		1s(A $_1$ ) $\rightarrow$ 5f $_0$	1s(A $_1$ ) $\rightarrow$ 5f $_0$	38.01 [9]



TABLE III. (Continued.)

Donor lines (meV) & in $\text{cm}^{-1}$		Transition/Line/Band assignment	Transition/Line/Band assignment and energy	
@5K	@ 20K / @ 35 K	(this work) Li	(previous reports)	
306.57 $\text{cm}^{-1}$				
38.20	38.23 /	$1s(A_1) \rightarrow 5p_{\pm}$	$1s(A_1) \rightarrow 5p_{\pm}$	38.20 [9]
308.12 $\text{cm}^{-1}$			gr.st. $\rightarrow 5p_{\pm}$	38.21 [12]
38.41		$1s(A_1) \rightarrow 5f_{\pm}$	$1s(A_1) \rightarrow 5f_{\pm}$	38.38 [9]
309.81 $\text{cm}^{-1}$				
38.59		$1s(A_1) \rightarrow 6p_{\pm}$	gr.st. $\rightarrow 6p_{\pm}$	38.584 [12]
311.13 $\text{cm}^{-1}$			$1s(A_1) \rightarrow 6p_{\pm}$	38.60 [9]
38.81		$1s(A_1) \rightarrow 6h_{\pm}$		
313.26 $\text{cm}^{-1}$		$1s(A_1) \rightarrow 7h_{\pm}$		
39.02				
				39.41(7) [5]
39.67		$E_i$		39.67 [9]
				39.67 [12]

the spectra, including  $d$ -type and Rydberg-like high excited states.

## II. EXPERIMENT

### A. Sample preparation and characterization

Si samples in this study were made from high-purity FZ-grown crystals doped from the melt using the so-called pedestal technique [15]. This method was used, because of the high vapor pressure of Li in Si, which is  $\sim 1.38$  bar. The dopant pill was located in an axial hole on the top of the feed rod being always covered with the melt and gradually evaporated with rising temperature of the pill's bottom. In this way, the melt zone was steadily doped by the Li vapor. To improve the radial and axial homogeneity of the doping concentration, a couple of pills were usually loaded in an initially undoped Si ingot. A weak axial Li gradient was determined by four-point probe resistivity measurement. It was used to obtain a set of concentrations between  $10^{15}$  and  $10^{16} \text{ cm}^{-3}$  (Table II). The samples with different concentrations are critically important for this investigation, because there is a trade-off between detection of impurity transitions with low oscillator strengths and concentration broadening of Li-related absorption lines. To observe unsaturated absorption in the strongest Li transitions, a low-doped Si:Li crystal was grown using additional float-zone run of the moderately doped Si:Li crystal No. V492 as starting material. The samples have optically polished facets with sizes ranging from  $7 \times 7$  to  $10 \times 10 \text{ mm}^2$  and thicknesses from  $\sim 0.5$  to  $\sim 1$  mm. The large facets of the samples were wedged to  $2^\circ$  or  $3^\circ$  depending on the sample thickness.

### B. Infrared absorption spectroscopy

Impurity absorption spectroscopy was performed using a Vertex 80v infrared Fourier-transform spectrometer (Bruker GmbH) equipped with a helium-flow cryostat (Janis). The temperature was varied from  $\sim 80$  K down to  $\sim 5$  K, and measured by a pair of thermosensors attached to the cold

finger close to the samples. The Si:Li samples were glued to the cold finger by a silver paint (RS Components). The resolution of the spectrometer was  $0.13 \text{ cm}^{-1}$  (photon energy:  $16 \mu\text{eV}$ ). The measured transmission spectra were converted to absorption spectra assuming single-path light propagation and calibrated to the multiphonon absorption bands of undoped Si (see Ref. [16] for details of the procedure).

The transmission spectra were taken at temperatures from  $\sim 5$  to  $\sim 80$  K with steps of 1.5 K (at lower temperatures) or 5 K (Fig. 2). Typical spectra of Si:Li samples (Figs. 2 and 3) present several types of impurity intracenter transitions: The lines observed at  $T = 5$  K in the spectral range 19–33 meV are intracenter transitions of the isolated Li donor; the lines in the range 18–40 meV are intracenter transitions of the Li-O donor

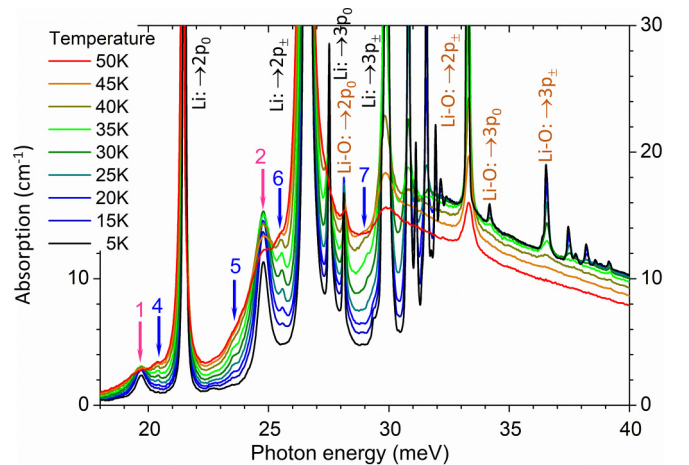


FIG. 2. Overview of absorption spectra of the Si:Li sample No. 482-3 at several different lattice temperatures, showing overlap of Li and Li-O intracenter transitions. Strongest intracenter absorption transitions of Li and Li-O donors from their ground states are marked by arrows with a final state of the transition. Numbered lines are those exhibiting increasing absorption with increasing temperature from 4.7 K. For their assignment please see the discussion in the main text.

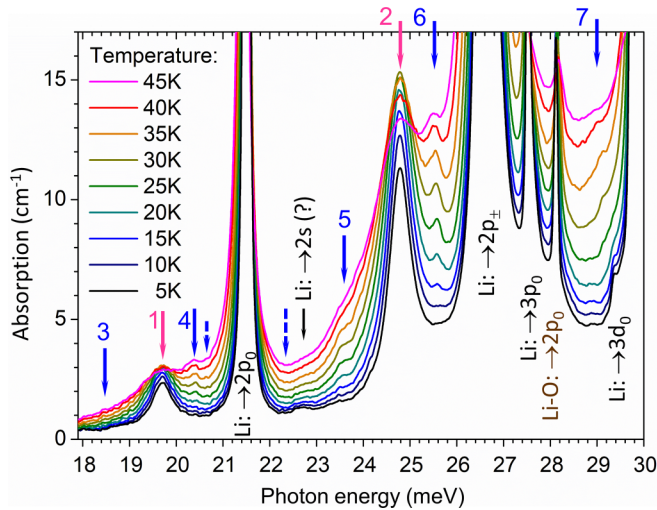


FIG. 3. Absorption spectra of Si:Li sample No. 482-3 at different temperatures (expanded view of Fig. 2 in the range of thermally induced transitions). Weak transitions (dashed arrows) vanish with increasing temperatures; other transitions (numbered arrows) reach their maximum at elevated temperatures.

complex. A few spectral features have vanishing intensities (Fig. 3) and their origin cannot be identified appropriately: We speculate that they have an origin somewhat similar to previously reported higher-energy Li-related centers, with Li coupled to several oxygen atoms [6,9] while the lines at lower energies might be assigned to Li molecules/clusters, e.g., similar to those assumed in Si doped by interstitial magnesium [17].

The strongest lines of Li and Li-O centers exhibit saturated absorption (optical density  $OD \gg 1$ ) in moderately doped samples (donor concentration exceeds  $10^{15} \text{ cm}^{-3}$ ). In addition, several weak transitions can be observed in the absorption spectra and evaluated using these samples.

There are two broad lines No. 1 and No. 2; both are 1.82(2) meV to the low-energy site of the Li transitions from its ground state into the  $2p_0$  and  $2p_{\pm}$  states (Fig. 3). Both lines have a similar evolution with temperature (Fig. 4): They have nonvanishing intensities at the lowest temperatures of our experiment, exhibit a slight enhancement at about 21 K, and decay above.

This indicates on transitions from excited states which have a small energy separation ( $\sim kT$ ) to the ground state. We note that a similar peak temperature of  $T = 22.5 \text{ K}$  was found for transitions from the thermally populated excited  $1s$  state in boron-doped diamond with a spin-orbit splitting of about 2 meV [18]. The centers of the lines No. 1 and No. 2 remain unchanged up to temperatures of almost 40 K. Their further evolution cannot be determined accurately due to the line's weak intensity and strong increasing neighboring Li lines from the ground state. The peak value of the absorption ratio of line No. 2 to line No. 1 is 5.4(4) (see Fig. 5), while the same for the ground state  $\rightarrow p_{\pm}$  and ground state  $\rightarrow p_0$  lines of the Li donor varies between 5 and 6. The linewidth of lines No. 1 and No. 2 does not change with concentration of Li donors as strongly as that of intracenter Li transitions from the ground state. It varies from 340  $\mu\text{eV}$  (full width at half maximum FWHM, 10 K, No. V467 samples series, line No. 2)

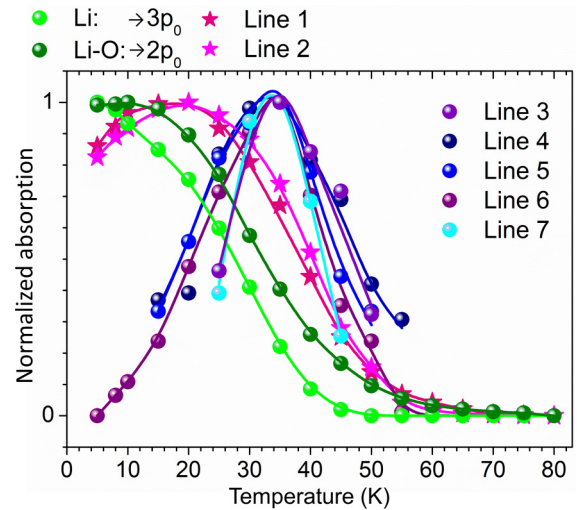


FIG. 4. Temperature dependences of intracenter transitions of Li-related donors in the No. 467-4 sample. For isolated Li and Li-O complexes, the unsaturated transitions (i.e., from their ground states into the  $3p_0$  and  $2p_0$  states) are taken for comparison. Note that an accurate determination of the absorption of lines No. 3, No. 4, and No. 7 is limited due to close-by weak lines which overlap with increasing temperature (see Fig. 3).

up to 450  $\mu\text{eV}$  in moderately doped samples, while all ground state  $\rightarrow np_{\pm}$  transitions have FWHM within 25–41  $\mu\text{eV}$  (Fig. 6). The peak value of the absorption cross-sections ratio of “line No. 2 to the unsaturated absorption on the ground state  $\rightarrow 3p_0$  transition (e.g.,  $1.13 \times 10^{-15} \text{ cm}^2$  (max at 30 K)/  $1.56 \times 10^{-14} \text{ cm}^2$  (max at 5 K) for No. 467-4) is about an order of magnitude smaller than that of the same transitions of group-V donors in Si without spin-orbit splitting of the ground state (e.g.,  $4.83 \times 10^{-15} \text{ cm}^2$  (max at 50 K)/  $4.37 \times 10^{-15} \text{ cm}^2$  (max at 5 K) for the line  $1s(T_2) \rightarrow 2p_{\pm}$  to the  $1s(A_1) \rightarrow 3p_0$  in Si:P). All these factors point strongly to a specific broadening mechanism of these transitions. This could be related to

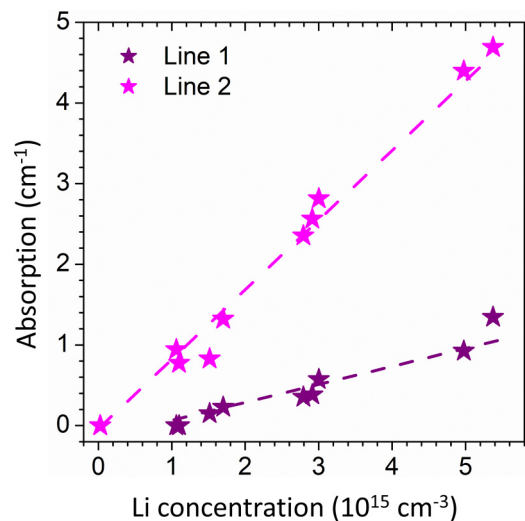


FIG. 5. Absorption coefficients of lines No. 1 and No. 2 in Si:Li samples with different Li concentrations at 5 K. Note the linear dependences of the transition intensities on the concentration of the isolated Li donor.

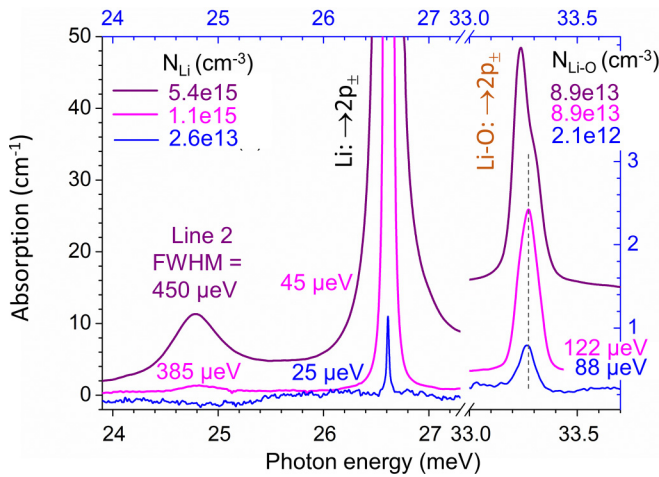


FIG. 6. Absorption spectra of differently doped samples (purple: No. 482-3, pink: No. V467-1, blue: No. 2V3951E) at 5 K around Li-related donor transitions, which terminate in the  $2p_{\pm}$  state. Note the different linewidths of the Li and Li-O donors in the low-doped sample No. 2V3951E) as well as the low-energy component of the  $1s(A_1) \rightarrow 2p_{\pm}$  transition of Li-O complex arising in the heavy-doped sample No. V482-3.

relatively strong impurity-phonon interaction, similar to those found for anomalous broad lines caused by a specific donor-phonon resonant interaction in  $n$ -Si [19]. Donor interaction with intervalley  $f$ -TA phonons in Si was argued to control intracenter relaxation of the lowest excited  $p$  states [20]. Considering the vicinity of these intracenter transitions to the energies of  $f$ -TA phonons in Si, which are  $\sim 18.4$  and  $\sim 25.4$  meV [21], we speculate that such a quasiresonant interaction could be a reason for enhanced line broadening of the excited state  $\rightarrow np_{\pm}$  transitions of isolated Li donors.

The absorption measured at the line centers increases linearly with the Li concentration in the samples (Fig. 5). Note that for donors formed by complexes of atoms the concentration follows a higher-order power law, for example the third power for thermal, oxygen-based donors [22].

Lines No. 4, No. 6, and No. 7 are 1.1(1) meV on the low-energy side of the Li transitions from its ground state into  $2p_0$  and  $2p_{\pm}$  states and 7.70(1) meV of the Li-O transitions from its ground state into  $2p_0$ ,  $2p_{\pm}$ , and  $3p_{\pm}$  states. They exhibit similar temperature dependences in the absorption spectra (Figs. 2 and 5); i.e., they were not detected at the lowest lattice temperature and reach its maximum intensity at 34(2) K. This peak temperature fits well to the trend of the valley-orbit splitting of all hydrogen-like donors in Si (Fig. 7) [23]. Their linewidths are similar and increase with temperature like intracenter transitions from the ground states of the donors.

There is a clear attribute that can be unambiguously used for separation of Li and Li-O intracenter transitions originating from their ground states (Fig. 8). The transitions of the Li-O center [ground state is a  $1s(A_1)$  level] follow a temperature evolution trend similar to that of group-V substitutional donors in Si [24] as well as the strongest  $1s(A_1) \rightarrow 2p_{\pm}$  transition of residual phosphorus in our samples, namely, their energy exhibits a blueshift with increase of lattice temperature. In contrast, intracenter transitions of the Li center

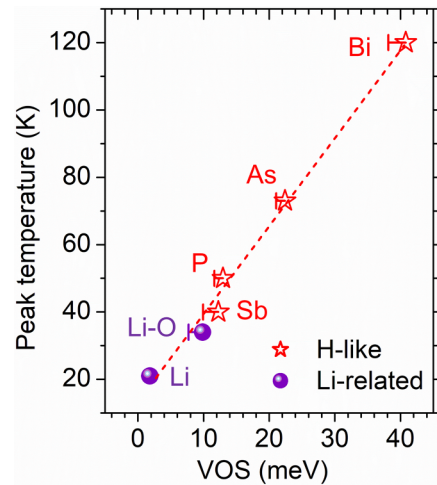


FIG. 7. Temperatures of peak intensities of intracenter transitions of donors in Si vs their ground state's VOS energy (for Li: energy between ground- and the lowest excited state). Hydrogen-like transitions are for substitutional group-V donors [23]; error bars are the gaps  $\Gamma_3 - \Gamma_5$ .

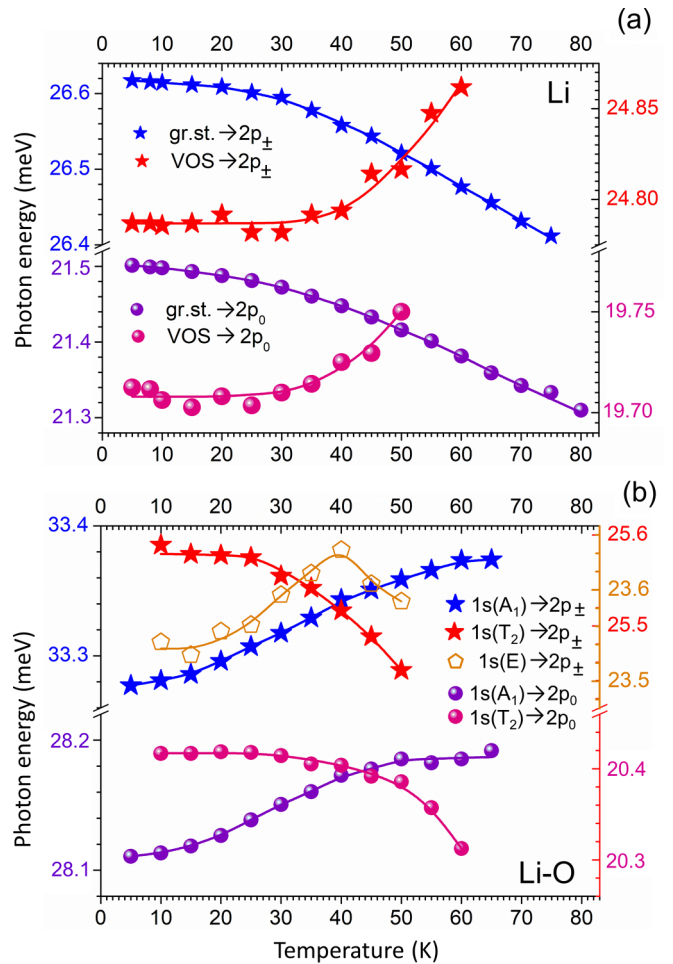


FIG. 8. Temperature evolution of energy of intracenter transitions in Si:Li samples (the data are for the No. 467- and No. V482-series). Note the opposite temperature gradients for similar types of intracenter transitions of isolated Li and Li-O complex donors.





absorption spectra. Also, the transition into the even-parity  $3d_0$  state was observed in Si:Li crystals. The observed transitions are summarized in Table III, where the transition energies as well as assignment of the involved levels are compared with previously reported ones.

There are two transitions in the spectra of moderately doped Si:Li samples whose energy would fit well with the calculated  $2s$  states (binding energy around 10 meV) of shallow substitutional donors in Si [28] assuming that they belong to the Li-O center. However, we do not speculate on their assignment. There is also a line at the low-energy slope [ $\sim 0.22 \text{ cm}^{-1}/28(5) \mu\text{eV}$ ] of the  $1s(A_1) \rightarrow p_0; p_{\pm}$  transitions of the Li-O center. It has a strong dependence on the concentration of Li in the samples: In many samples its absorption peak is lower than those of  $1s(A_1) \rightarrow p_0; p_{\pm}$  transitions for the less-doped series No. 467 and exceeds the latter for the heavily doped series No. 482. We do not have a tentative assignment for this exotic center.

### III. DISCUSSION

One of the challenges of the interpretation of Li-related spectra is overlapping transitions of isolated Li donor and Li-O complex, which always appear together in the spectra. The relative intensities of their transitions depend mostly on the initial Si crystal properties. In most cases Li-related complexes exhibit a significantly lower intensity. In the pioneering optical studies of Si:Li [5], the choice of initial low-oxygen FZ-grown and moderate-oxygen Cz-grown Si crystals allowed for a reasonable separation of Li and Li-O at high densities of the diffused Li. Later, a similar study [9] has shown that at lower Li concentrations such a separation becomes difficult: It was found that due to “aggressive” bonding to oxygen, a pronounced Li-O complex occurs even in assumed low-oxygen FZ-grown samples. In both of these reports, one can find ambiguous assignments of several observed absorption lines: (i) In Cz-grown Si:Li, line  $x_1$  at 26.63(2) meV was assigned to the Li-O transition series [5], while it is very likely the ground state  $\rightarrow 2p_{\pm}$  transition of isolated Li; (ii) the transition at 28.10(3) meV, assigned to excited state  $\rightarrow 3p_{\pm}$  isolated Li transition at  $\sim 20$  K [8,9], is very likely the ground state  $\rightarrow 2p_0$  transition of a Li-O complex, because otherwise one should observe in the same spectrum the excited state  $\rightarrow 2p_0$  Li transition, which has a somewhat larger oscillator strength and which is less affected by the lattice temperature; (iii) in order to derive the conclusion on a thermally induced transition at about 24.8 meV, the authors compared the spectra at  $\sim 5$  K of the sample with a Li concentration of  $\sim 2 \times 10^{14} \text{ cm}^{-3}$  with that of another, heavily doped sample ( $\sim 1.1 \times 10^{15} \text{ cm}^{-3}$ ) at a temperature of  $\sim 20$  K [8]. However, in the present work we show that such a difference in concentration of Li enables the observation of this spectral feature already at low temperature (5 K); and (iv) although the  $\sim 24.8$  meV transition was assigned at the elevated temperature  $\sim 20$  K in Ref. [5], some spectra in that work show a broad feature around 25 meV also at liquid helium cooling.

These uncertainties reduce the number of arguments about the “inversed”  $1s(A_1)$  ground state to the only temperature-

enhanced transition at  $\sim 24.8$  meV [5]. This transition has a much broader FWHM, several times larger than those from the next Li transition from the ground state into the  $2p_{\pm}$  level (Fig. 7). Apparently, this observation was not taken into account in previous studies using instruments with lower spectral resolution [5]. But, it was clearly observed in high-resolution measurements in Ref. [8]. Such a broad linewidth was probably the reason to assign this transition to the one terminating in the  $2s$  state [6] that would give a correct order of magnitude for the theoretical estimate of the  $2s$  state [28], but is not suitable for the temperature evolution of its absorption spectrum. The temperature evolution and peak intensity indicate a very small energy gap to the ground state of the donor. Since the next broad transition appears at the same energy shift as the ground state  $\rightarrow 2p_0$  transition, its assignment to thermally populated state(s) of the Li center is well justified.

Note that the main argument to assign the ground state to the fivefold multiplet  $1s(E + T_2)$ , namely the appearance of the central component of the transitions terminating in the excited  $p$  states [5,8], is not unambiguous: The same set of stress-split transitions would be formed if the ground state were a fourfold multiplet  $1s(A_1 + T_2)$  in the  $T_d$  symmetry or for instance if assuming a nonvanishing spin-orbit splitting (SOS) of the  $1s(T_2 : \Gamma_5)$  state, which would form the components  $1s(T_2 : \Gamma_8)$  and  $1s(T_2 : \Gamma_7)$  [29]. In the latter case the SOS  $1s(T_2)$  state would be sufficient to explain piezospectroscopic observations. We note also that a fine spin-orbit coupling of the Li ground state was reported from ESR study of isotopically enriched  $^{28}\text{Si}:\text{Li}$  [14]. Concluding here, there is no unambiguous argument for an “inverted” VOS, i.e., that the  $1s(A_1)$  state has lower binding energy than the  $1s(E)$  [5,9].

The excited states in the broad band of the Li donor might have an unusual structure. It is not obvious that other symmetry configurations of the Li donor may occur, for instance due to Jahn-Teller distortion, like in diamond [30]. A similar phenomenon can be expected for an interstitial Li donor. Assuming  $T_d$  symmetry of the ground Li state, a multiplet may consist of unresolved  $\Gamma_1$  and  $\Gamma_3$  components of the excited multiplet (Fig. 1). For an alternative symmetry of Li donor, there might be a set of singlet and doublet states in the multiplet. A  $1s(E)$  ground state was found in the model of the dielectric screening effect on the core charge-density impurity, developed by Nara and Morita [3]. This finding is unusual in the frame of the EMT approximation. Applying their approach developed for donors in Si [31] to isolated interstitial Li, they found strong dependences of the chemical shift for the components of the Li ground state on the parameter  $r_0$ , describing spatial distribution of Li in the Si lattice. For two considered symmetry types of the ground state,  $T_d$  and  $D_{3d}$ , their simulations resulted in the  $\Gamma_3$ -type ground state [ $1s(E)$ ] for large  $r_0$  while  $T_2$  and  $A_1$  levels become excited states and may have diverse relative energies [3].

The ESR studies have shown that there is a fine structure of the ground state: the splitting “within  $0.1\text{--}0.2 \text{ cm}^{-1}$ ” ( $12\text{--}25 \mu\text{eV}$ ) for assumed unresolved components of the Li ground state [7]. Note that such relatively small exchange energy would not be sufficient to explain the FWHM of the excited VOS state band, but would be reasonable for the spin-orbit split ground state if assuming it to be a  $\Gamma_5$  type.

Concluding here, we cannot assign the valley-orbit splitting of the Li donor to the energy gap between the  $1s(A_1)$  and  $1s(E)$  states, since the symmetry of the components is not determined in our study. Instead, we suppose the chemical shift (energy gap between ground state and the excited states split off by valley-orbit interaction) to be a valley-orbit-split energy.

The absolute energy of the transitions for both Li and Li-O centers in our study agrees better with those obtained by photothermal ionization spectroscopy [12]. The measurements with a “stress-free” mounting with only a “point” contact to the cold finger in the cryostat in the studies reported in Refs. [5,9] are apparently slightly temperature shifted (Table II). We point out that for the optically thick samples (if OD at strong intracenter transitions is much larger than 1) determination of the impurity line center is not accurate. Therefore, we rely on the low-doped samples for the transitions with oscillator strengths above 0.02 [32].

One may argue that the doping of Si with Li from melt, as performed in this study, provides better homogeneity of Li donors when compared with diffusion doping—the technique used in most of the previous studies. However, the optical properties of the Li centers obtained by pedestal techniques appear to be identical to those reported previously. At the same time we do not exclude that a better quality of the *in situ*-doped Si:Li crystals enables observations of weaker transitions of Li and Li-O center, which lead to a modified interpretation of their VOS. It should be noted that other Li-O related donors observed in Cz-grown Si:Li were not detected in our samples.

#### IV. CONCLUSIONS

The study of the temperature evolution of absorption spectra of Li-related donors in Si revealed a few important observations and leads to updated constraints on the valley-orbit splitting of the ground states:

(i) The Li-O donor in Si exhibits a temperature evolution very similar to substitutional group-V donors in Si. It has a valley-orbit splitting of the ground state, which is slightly less than that for antimony, the shallowest substitutional donor in Si. Its  $\Gamma_3$  ground state is the shallowest [29.804(5) meV] of all known single-electron shallow donors [1] (with the exception of thermal donors in Si) while the  $\Gamma_3 - \Gamma_5$  splitting ( $\sim 2.16$  meV) is within the range of experimentally observed values for group-V donors in Si [23];

(ii) The isolated Li donor in Si exhibits an opposite temperature evolution of the transitions from its ground state when compared with those of a Li-O center. This donor exhibits a very low valley-orbit splitting (the chemical shift in this case) of the ground state of about 1.82 meV, the smallest of all single-electron shallow donors in Si. Its ground state is apparently similar to a  $\Gamma_5$  type ( $T_d$ ) or alternatively to  $\Gamma_5 + \Gamma_1$  type ( $T_d$ ), while VOS state(s) are lifted up, making many of its properties different from donors in Si. The intracenter optical transitions from the thermally populated VOS state(s) are anomalously broadened. and

(iii) High-quality *in situ*-doped FZ-grown Si:Li crystals enabled the observation of many states with very low oscillator strengths, including those into even-parity ( $3d_0$ ) as well as high excited levels of donors (up to  $7h_{\pm}$ ), often called Rydberg-type (-like) states. Note that such states were resolved previously only in the ultrahigh-purity natural Si [26]. Due to their narrow transition linewidths it was possible to observe these high excited states. This is unexpected for randomly distributed interstitial centers in Si lattice.

#### ACKNOWLEDGMENTS

The authors thank Dr. N. Notzel and Dr. H. Riemann for technical support and Professor A. A. Ezhevskii for the fruitful discussion.

- 
- [1] A. K. Ramdas and S. Rodriguez, Spectroscopy of the solid-state analogues of the hydrogen atom: Donors and acceptors in semiconductors, *Rep. Prog. Phys.* **44**, 1297 (1981).
  - [2] R. A. Faulkner, Higher donor excited states for prolate-spheroid conduction bands: A reevaluation of silicon and germanium, *Phys. Rev.* **184**, 713 (1969).
  - [3] H. Nara and A. Morita, Chemical splitting of ground state of lithium donor in silicon, *J. Phys. Soc. Jpn.* **23**, 831 (1967).
  - [4] G. Feher, Electron spin resonance experiments on donors in silicon. I. Electronic structure of donors by the electron nuclear double resonance technique, *Phys. Rev.* **114**, 1219 (1959).
  - [5] R. L. Aggarwal, P. Fisher, V. Mourzine, and A. K. Ramdas, Excitation spectra of lithium donors in silicon and germanium, *Phys. Rev.* **138**, A882 (1965).
  - [6] T. E. Gilmer, Jr., R. K. Franks, and R. J. Bell, An optical study of lithium and lithium-oxygen complexes as donor impurities in silicon, *J. Phys. Chem. Solids* **26**, 1195 (1965).
  - [7] G. D. Watkins and F. S. Ham, Electron paramagnetic resonance studies of a system with orbital degeneracy: The lithium donor in silicon, *Phys. Rev. B* **1**, 4071 (1970).
  - [8] C. Jagannath and A. K. Ramdas, Piezospectroscopy of isolated lithium donors and lithium-oxygen donor complexes in silicon, *Phys. Rev. B* **23**, 4426 (1981).
  - [9] C. Jagannath, Z. W. Grabowski, and A. K. Ramdas, Linewidths of the electronic excitation spectra of donors in silicon, *Phys. Rev. B* **23**, 2082 (1981).
  - [10] B. Szablak and M. Altarelli, Electronic structure of lithium interstitials in Si, *Solid State Commun.* **37**, 341 (1981).
  - [11] R. Sauer, Optical determination of highly excited s-like donor states in silicon, *J. Lumin.* **12–13**, 495 (1976).
  - [12] Zhiyi Yu, Y. X. Huang, and S. C. Shen, New shallow donors in high-purity silicon single crystal, *Appl. Phys. Lett.* **55**, 2084 (1989).
  - [13] D. Karaiskaj, J. A. H. Stotz, T. Meyer, M. L. W. Thewalt, and M. Cardona, Impurity Absorption Spectroscopy in  $^{28}\text{Si}$ : The Importance of Inhomogeneous Isotope Broadening, *Phys. Rev. Lett.* **90**, 186402 (2003).
  - [14] A. A. Ezhevskii, A. P. Detochenko, S. A. Popkov, A. A. Konakov, A. V. Soukhorukov, D. V. Guseinov, D. G. Zverev, G. V. Mamin, N. V. Abrosimov, and H. Riemann, Spin relaxation

- times of donor centers associated with lithium in monoisotopic  $^{28}\text{Si}$ , *Solid State Phenom.* **242**, 322 (2005).
- [15] N. V. Abrosimov, N. Nötzel, H. Riemann, K. Irmscher, S. G. Pavlov, H.-W. Hübers, U. Böttger, P. M. Haas, N. Drichko, and M. Dressel, Silicon doped with lithium and magnesium from the melt for terahertz laser application, *Solid State Phenom.*, **131–133**, 589 (2008).
- [16] S. G. Pavlov, L. M. Portsel, V. B. Shuman, A. N. Lodygin, Yu. A. Astrov, N. V. Abrosimov, S. A. Lynch, V. V. Tsyplenkov, and H.-W. Hübers, Infrared absorption cross sections, and oscillator strengths of interstitial and substitutional double donors in silicon, *Phys. Rev. Mater.* **5**, 114607 (2021).
- [17] S. G. Pavlov, Yu. A. Astrov, L. M. Portsel, V. B. Shuman, A. N. Lodygin, N. V. Abrosimov, and H.-W. Hübers., Magnesium-related shallow donor centers in silicon, *Mater. Sci. Semicond. Process.* **130**, 105833 (2021).
- [18] S. G. Pavlov, D. D. Prikhodko, S. A. Tarelkin, V. S. Bormashov, N. V. Abrosimov, M. S. Kuznetsov, S. A. Terentiev, S. A. Nosukhin, S. Yu. Troschiev, V. D. Blank, and H.-W. Hübers, Resonant boron acceptor states in semiconducting diamond, *Phys. Rev. B* **104**, 155201 (2021).
- [19] A. Onton, P. Fisher, and A. K. Ramdas, Anomalous Width of Some Photoexcitation Lines of Impurities in Silicon, *Phys. Rev. Lett.* **19**, 780 (1967).
- [20] V. V. Tsyplenkov, E. V. Demidov, K. A. Kovalevsky, and V. N. Shastin, Relaxation of excited donor states in silicon with emission of intervalley phonons, *Semiconductors* **42**, 1016 (2008).
- [21] M. Asche and O. G. Sarbei, Electron–phonon interaction in n-Si, *Phys. Status Solidi* **103**, 11 (1981).
- [22] W. Kaiser, H. L. Frisch, and H. Reiss, Mechanism of the formation of donor states in heat-treated silicon, *Phys. Rev.* **112**, 1546 (1958).
- [23] S. G. Pavlov, N. V. Abrosimov, V. B. Shuman, L. M. Portsel, A. N. Lodygin, Yu. A. Astrov, R. Kh. Zhukavin, V. N. Shastin, K. Irmscher, A. Pohl, and H.-W. Hübers, Even-parity excited states in infrared emission, absorption, and Raman scattering spectra of shallow donor centers in silicon, *Phys. Status Solidi B* **256**, 1800514 (2019).
- [24] S. G. Pavlov, N. V. Abrosimov, and H.-W. Hübers, Thermal corrections to the valley-orbit split states of shallow donors in silicon (unpublished).
- [25] C. Y. Cheung and R. Barrie, The temperature dependence of the energy levels of shallow donor impurities in silicon, *Can. J. Phys.* **45**, 1421 (1967).
- [26] M. Steger, A. Yang, D. Karaickaj, M. L. W. Thewalt, E. E. Haller, J. W. Ager, III, M. Cardona, H. Riemann, N. V. Abrosimov, A. V. Gusev, A. D. Bulanov, A. K. Kaliteevskii, O. N. Godisov, P. Becker, and H.-J. Pohl, Shallow impurity absorption spectroscopy in isotopically enriched silicon, *Phys. Rev. B* **79**, 205210 (2009).
- [27] B. Pajot, J. Kauppinen, and R. Anttila, High resolution study of the group V impurities absorption in silicon, *Solid State Commun.* **31**, 759 (1979).
- [28] Y.-C. Chang, T. C. McGill, and D. L. Smith, Model Hamiltonian of donors in indirect-gap materials, *Phys. Rev. B* **23**, 4169 (1981).
- [29] A. J. Mayur, M. D. Sciacca, A. K. Ramdas, and S. Rodriguez, Redetermination of the valley-orbit (chemical) splitting of the  $1s$  ground state of group-V donors in silicon, *Phys. Rev. B* **48**, 10893 (1993).
- [30] R. J. Eyre, J. P. Goss, P. R. Briddon, and J. P. Hagon, Theory of Jahn–Teller distortions of the P donor in diamond, *J. Phys.: Condens. Matter* **17**, 5831 (2005).
- [31] A. Morita, M. Azuma, and H. Nara, Theory of impurity levels, *J. Phys. Soc. Jpn.* **17**, 1570 (1962).
- [32] I. L. Beñikhes and Sh. M. Kogan, Donors in multivalley semiconductors in the zero-radius center-cell approximation, *Zh. Eksp. Teor. Fiz.* **93**, 285 (1987) [*Sov. Phys. JETP* **66**, 164 (1987)].